Journal of Food Engineering 327 (2022) 111060

Contents lists available at ScienceDirect

Journal of Food Engineering

journal homepage: www.elsevier.com/locate/jfoodeng

Coefficient of restitution of kiwifruit without external interference

Zhenchao Wu [a], Guo Li [a], Ruizhe Yang [a], Longsheng Fu [a,b,c,*], Rui Li [a], Shaojin Wang [a,d]

[a] College of Mechanical and Electronic Engineering, Northwest A&F University, Yangling, Shaanxi, 712100, China
[b] Key Laboratory of Agricultural Internet of Things, Ministry of Agriculture and Rural Affairs, Yangling, Shaanxi, 712100, China
[c] Shaanxi Key Laboratory of Agricultural Information Perception and Intelligent Service, Yangling, Shaanxi, 712100, China
[d] Department of Biological Systems Engineering, Washington State University, 213 L.J. Smith Hall, Pullman, WA, 99164-6120, USA

ARTICLE INFO

Keywords:
Coefficient of restitution
Fruit-fruit collision
Kiwifruit
Firmness
Collision velocity
Total bruise volume

ABSTRACT

Coefficient of restitution (CoR) is an important parameter required to simulate kinematics and collision physics of various materials using simulation software. Most current methods for determining the CoR of fruit-fruit collision (FFC) may be interfered by other colliding objects. In this study, a platform was designed to realize the FFC of kiwifruit without introducing other colliding objects, where influences of different factors (including ripening time, collision velocity, and fruit collision posture) on the CoR were studied. Total bruise volume (TBV), the sum of two fruit bruise volumes after the FFC, was measured and correlated with the CoR. Results showed that the CoR on early ripening time was large and its standard deviation was small, but opposite on late ripening time. The CoR of the FFC decreased with collision velocity increasing, except for the late ripening time. The fruit collision posture had also affect on the CoR because the difference in the rotation angle of the fruit during the FFC. Moreover, the TBV decreased with increasing of the CoR and was 0 mm^3 when the CoR exceeded 0.58. The CoR could not only be an appropriate parameter to predict fruit damage and describe bruise initiation, but also be used for simulations on the early ripening time. This research will help establish a more accurate fruit model and thus designing optimal fruit post-harvesting and processing systems.

1. Introduction

Equipment of fruit industry could be designed by numerical techniques and its performance is important for orchard. From orchard to supermarket, fruit may pass through several processes such as sorting, storage and transportation (Lu et al., 2010). Efficiency of these processes has a significant impact on orchard profitability, which requires equipment employed in processes' handling to be designed well (Bader and Rahimifard, 2020; Delpino-Rius et al., 2018; Rojas et al., 2016; Van Zeebroeck et al., 2008; Wu et al., 2021).

Numerical techniques, such as simulation software, have been widely used in designing and developing equipment, which allow detailed analyses on them. Discrete element method (DEM), one of the most common numerical techniques, could specifically apply to simulate kinematics of various materials. Zhao et al. (2019) obtained motion law of Lycium barbarum in horizontal airflow and designed winnowing equipment with 89.74% cleaning rate by DEM. Van Zeebroeck et al. (2008) demonstrated DEM for simulating damage to apples stored in bulk bins during passage of a truck over a speed bump, which showed that higher truck loads lead to less damage. Therefore, simulation software has great potential to improve equipment design and predict mechanical damage of fruit.

Coefficient of restitution (CoR) is one of the most important parameters required to simulate kinematics and collision physics of various materials in DEM simulation software. EDEM (DEM solution Ltd., Edinburgh, UK) has been widely used to simulate motion process of materials and establish parametric models (Barnabé et al., 2018; Kanakabandi and Goswami, 2019; Rossow and Coetzee, 2021; Tan et al., 2021). Mechanical damage as well as other affects in fruit cause lower selling prices and generate loss for fruit growers (Komarnicki et al., 2017a). Fruit damage assessment studies can contribute to reduce losses among fruit growers and production costs (Komarnicki et al., 2017b; Stopa et al., 2018). Characteristics of fruit motion and damage prediction during apple handling have been investigated by changing the CoR in DEM simulations (Van Zeebroeck et al., 2006). Therefore, the CoR is not only an important parameter for simulation software but also an appropriate parameter for predicting the fruit damage.

Pendulum method and drop method have been widely used to realize fruit-fruit collision (FFC) to study the CoR. In the pendulum method, the fruit was attached to the end of string and its movement was realized by

* Corresponding author. College of Mechanical and Electronic Engineering, Northwest A&F University, Yangling, Shaanxi, 712100, China.
E-mail address: fulsh@nwafu.edu.cn (L. Fu).

https://doi.org/10.1016/j.jfoodeng.2022.111060
Received 15 December 2021; Received in revised form 26 February 2022; Accepted 15 March 2022
Available online 17 March 2022
0260-8774/© 2022 Elsevier Ltd. All rights reserved.

exerting a force perpendicular to the direction of the string. Due to binding force of string, the FFC could be achieved by changing the pendulum movement of the fruit (Fu et al., 2020; Pang et al., 1992; Van Zeebroeck et al., 2007a; Wang et al., 2019). In the drop method, a fruit is released to a plate with multiple fruit to achieve the FFC (Opara et al., 2007; Stropek and Gołacki, 2013; Studman et al., 1997) and is subjected to the plate's support force. Therefore, whether pendulum method or drop method, fruit may be interfered with by other colliding objects during the FFC.

The main objectives of this study were: (1) to realize the FFC without introducing other colliding objects; (2) to measure the firmness of kiwifruits in different ripeness; (3) to determine the CoR under different factors (including ripening time, collision velocity, and fruit collision postures); (4) to analyze relationship between the CoR and the TBV in different ripeness.

2. Materials and methods

2.1. Materials

'Hayward', which is the most popular kiwifruit cultivar in the local market, was used in the study. Fruit was grown in Meixian Kiwifruit Experimental Station (latitude: 34°07′39″N, longitude: 107°59′50″E, and 648 m in altitude) in Shaanxi province, China. To reduce the influence of mass on measurement of bruise volume, fruit was selected for mass between 85 and 100 g. Therefore, on Oct 12, 2020, 400 fresh fruit (91.8 ± 5.8 g) were hand-picked and tested for firmness, FFC and fruit bruise. Fruit was stored in an incubator (Jtone Electronic CO., Hangzhou, China) at 25 °C and 80% relative humidity. Fruit were randomly divided into three groups, one of which was taken out of storage every 4 d (Du et al., 2019). The first day of storage, same as the first day of picking, was defined as Day 0. The 4 d and 8 d of storage were defined as Day 4 and Day 8, respectively. More fruit were needed in each group because the results would be inaccurate if the fruit was bumped before FFC tests. Therefore, 100, 200 and 100 fruit were taken out on Day 0, Day 4 and Day 8, respectively.

2.2. Measuring fruit firmness

Firmness was measured by puncture tests on 60 fruit, where 20 fruit were randomly selected from each group. According to operation manual of texture analyzer (TA.XTC-18, Shbosin Corp., Shanghai, China), the fruit without fruit skin was punctured by TA/2 probe. Puncture velocity and puncture depth were 1 mm/s and 5 mm, respectively.

2.3. Determining CoR of fruit-fruit collision

2.3.1. Platform for fruit-fruit collision

A platform was designed to realize the FFC without introducing other colliding objects. Two arciform plates, both with fruit holder and distance adjuster, were installed on a supporting plate. Mirror at 135° to the supporting wall which attached the supporting plate by retainer plate. Fruit protector was located at the bottom of the platform and directly below the two arciform plates, as shown in Fig. 1.

Initial release point of fruit on the arciform plate could be altered by the distance adjuster before the FFC. Fruit would be released by the fruit holders after pressing the start button of controller. In the FFC, collision velocity could be changed by altering the initial release point of fruit. And collision angle of the FFC could be altered by angle adjuster and calibrated by protractor. Distance between the two arciform plates was 200 mm through a large number of preliminary experiments. There were 80 mm sponge and 20 mm wadding in fruit protector to prevent the fruit damage of subsequent collisions. A high-speed digital camera (OLYMPUS i-speed TR; Keymed 'Medical & Industrial Equipment' Co., Ltd., UK) was used to record the FFC.

2.3.2. Acquiring three-dimensional velocity of fruit based on mirror reflection

According to principle of mirror reflection, three-dimensional velocity of fruit before and after the collision was calculated by analyzing high-speed digital videos. Top view of the platform of the FFC was shown in Fig. 2a, which included a mirror and a supporting wall angled

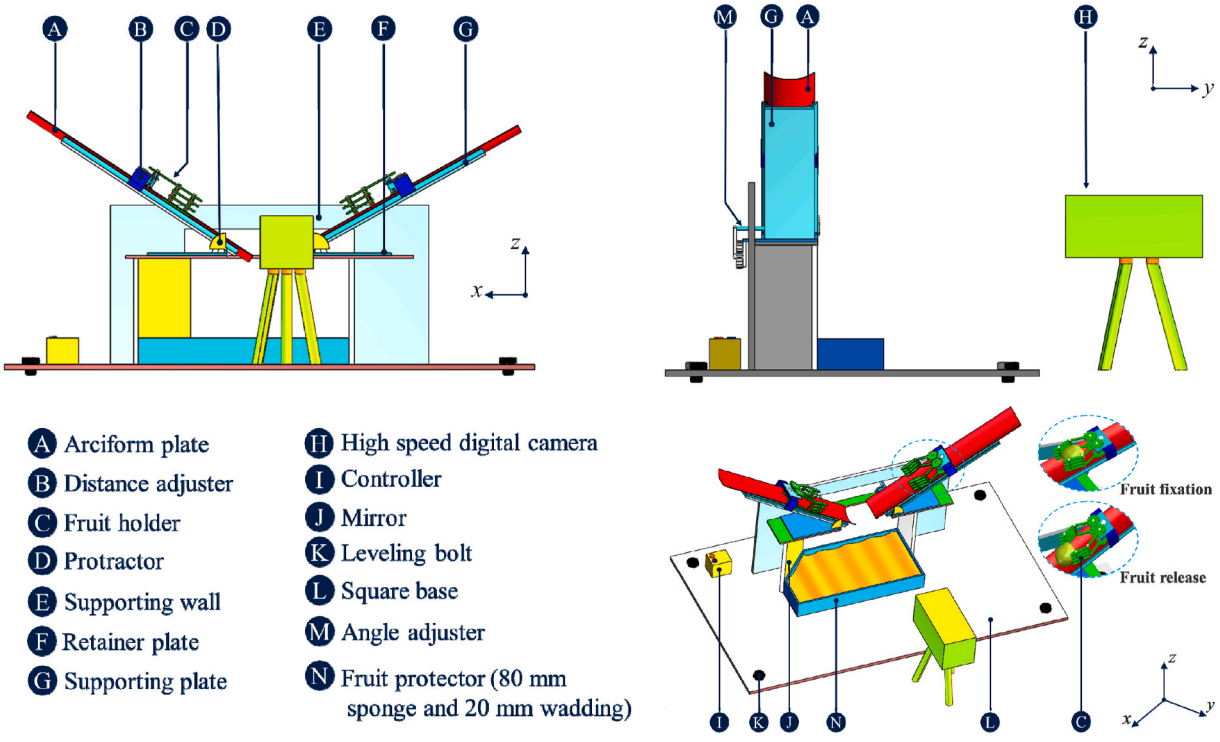


Fig. 1. Platform of fruit-fruit collision.

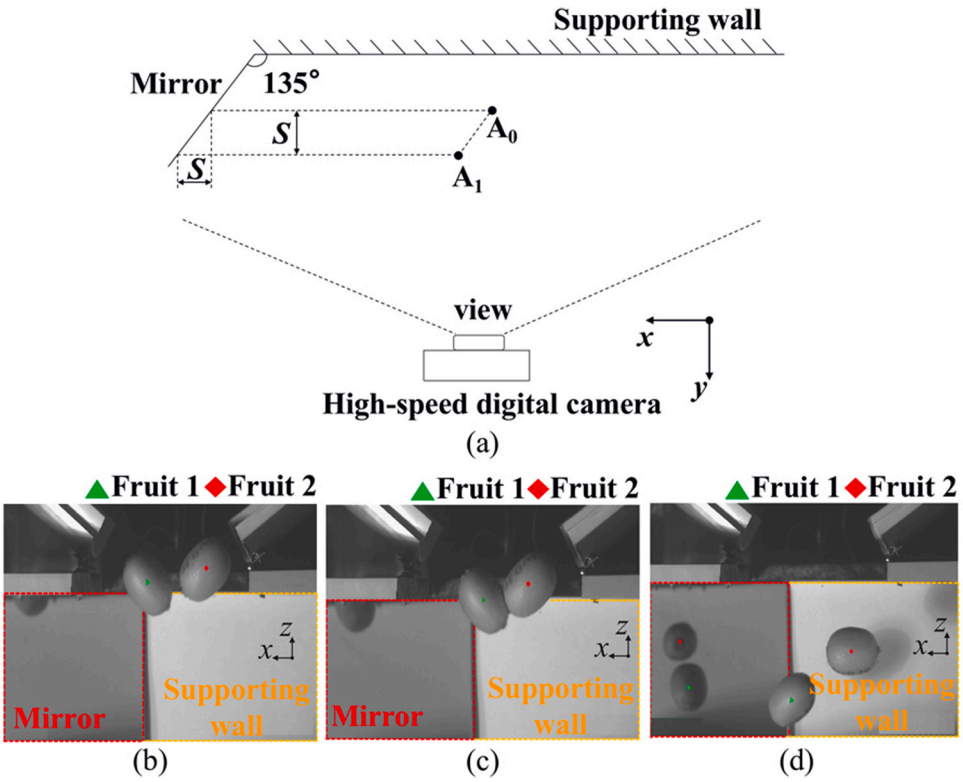


Fig. 2. Recording the FFC by a high-speed digital camera. (a) Image of the fruit reflected in the mirror (top view); (b) The FFC before collision; (c) The FFC during collision; (d) The FFC after collision.

at 135°. The high-speed digital camera was fixed vertically to record the trajectory of fruit. Resolution and frame rate of the high-speed digital camera were 1280 × 1024 pixels and 750 fps, respectively. FFC images from the high-speed digital camera were processed by i-SPEED Suite software. The distance was S when the fruit moved from point A_0 to point A_1 in the y-direction. Image coordinates of the fruit in the Z-X plane could be obtained directly from platform's front view, as shown in Fig. 2d. The image coordinates of the fruit in the Z-Y plane could also be obtained by mirror reflection.

2.3.3. Calculation of CoR

Theoretical formula of the CoR was deduced based on fruit deformation during collision, where both impact and rebound velocities were calculated from displacements before and after the collision. The CoR (e), as a parameter, could indicate recovery ability of colliding object during collision. In this study, its theoretical formula was deduced based on the fruit deformation during the collision. The fruit deformation only occurred during the collision, which made it difficult to obtain accurate deformation and velocity of a single fruit through the high-speed digital cameras. Therefore, both impact and rebound velocities were calculated from displacements before and after the collision.

(1) Theoretical formula of CoR

According to the fruit deformation during collision, the theoretical formula of the CoR (e) was deduced (Wang et al., 2018). To analyze the kinematics and collision characteristics of each fruit, the pair fruit in the ith FFC test were defined as fruit $i1$ and fruit $i2$, respectively. Deformations of fruit $i1$ and fruit $i2$ during the collision were δ_{i1} and δ_{i2}, respectively. The time of deformation process (t) was from 0 to T. Impact velocity vectors of fruit $i1$ and fruit $i2$ were $\boldsymbol{v}$impact $i1$ and $\boldsymbol{v}$impact $i2$, respectively, which were derivatives of the fruit deformation at $t = 0$ s, as shown in Eqs. (1) and (2). Similarly, rebound velocity vectors of fruit $i1$ and fruit $i2$ were $\boldsymbol{v}$rebound $i1$ and $\boldsymbol{v}$rebound $\boldsymbol{i}2$, respectively, which were derivatives of the fruit deformation at $t = \mathrm{T}$ s, as shown in Eqs. (3) and (4). Restoring forces of fruit $i1$ and fruit $i2$ were F_{i1} and F_{i2}, respectively, which were generated by the fruit deformation, as shown in Eqs. (5) and (6). Restoring forces along the contact force direction produced by the fruit deformation were equal in magnitude and opposite in direction, as shown in Fig. 3. Hence, the CoR of the FFC could be determined by Eqs. (7)–(9).

$$\mathrm{v}_{i1}(0) = \left.\frac{d\delta_{i1}}{dt}\right|_{t=0} = \mathrm{v}_{i1}^{\mathrm{impact}} \tag{1}$$

$$\mathrm{v}_{i2}(0) = \left.\frac{d\delta_{i2}}{dt}\right|_{t=0} = \mathrm{v}_{i2}^{\mathrm{impact}} \tag{2}$$

$$\mathrm{v}_{i1}(0) = \left.\frac{d\delta_{i1}}{dt}\right|_{t=\mathrm{T}} = \mathrm{v}_{i1}^{\mathrm{rebound}} \tag{3}$$

$$\mathrm{v}_{i2}(0) = \left.\frac{d\delta_{i2}}{dt}\right|_{t=\mathrm{T}} = \mathrm{v}_{i2}^{\mathrm{rebound}} \tag{4}$$

$$M_{i1}\mathrm{v}_{i1}^{\mathrm{rebound}} - M_{i1}\mathrm{v}_{i1}^{\mathrm{impact}} = \int_0^{\mathrm{T}} \mathrm{F}_{i1}dt \tag{5}$$

$$M_{i2}\mathrm{v}_{i2}^{\mathrm{rebound}} - M_{i2}\mathrm{v}_{i2}^{\mathrm{impact}} = \int_0^{\mathrm{T}} \mathrm{F}_{i2}dt \tag{6}$$

$$\mathrm{F}_{i1} = -\mathrm{F}_{i2} \tag{7}$$

$$m_{i1}\left(\mathrm{v}_{i1}^{\mathrm{rebound}} - \mathrm{v}_{i1}^{\mathrm{impact}}\right) = -\mathrm{m}_{i2}\left(\mathrm{v}_{i2}^{\mathrm{rebound}} - \mathrm{v}_{i2}^{\mathrm{impact}}\right) \tag{8}$$

$$e = \frac{\left|\left.\frac{d\delta_{i2}}{dt}\right|_{t=\mathrm{T}} - \left.\frac{d\delta_{i1}}{dt}\right|_{t=\mathrm{T}}\right|}{\left|\left.\frac{d\delta_{i2}}{dt}\right|_{t=0} - \left.\frac{d\delta_{i1}}{dt}\right|_{t=0}\right|} = \frac{\left|\left(\mathrm{v}_{i2}^{\mathrm{rebound}} - \mathrm{v}_{i1}^{\mathrm{rebound}}\right)\left(\mathrm{v}_{i2}^{\mathrm{rebound}} - \mathrm{v}_{i2}^{\mathrm{impact}}\right)\right|}{\left|\left(\mathrm{v}_{i2}^{\mathrm{impact}} - \mathrm{v}_{i1}^{\mathrm{impact}}\right)\left(\mathrm{v}_{i2}^{\mathrm{rebound}} - \mathrm{v}_{i2}^{\mathrm{impact}}\right)\right|} \tag{9}$$

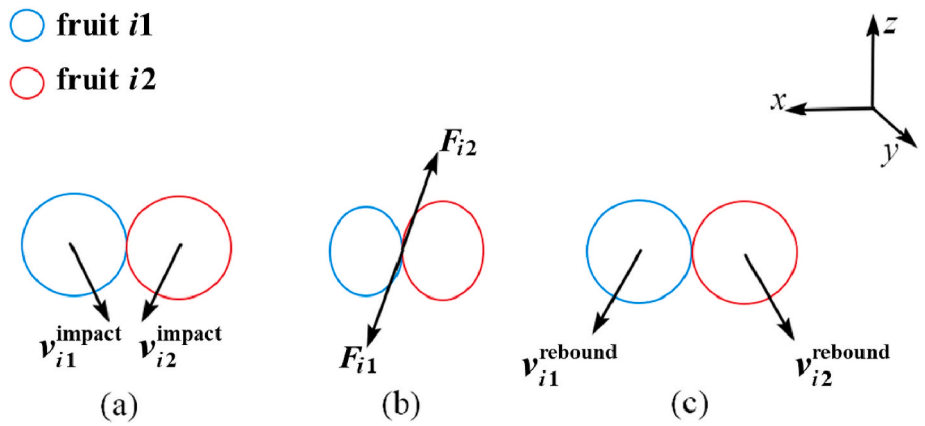


Fig. 3. FFC for the *i*th pair fruit in three-dimensions. (a) Fruit that impacted initially; (b) Fruit during collision; (c) Fruit that rebounded initially.

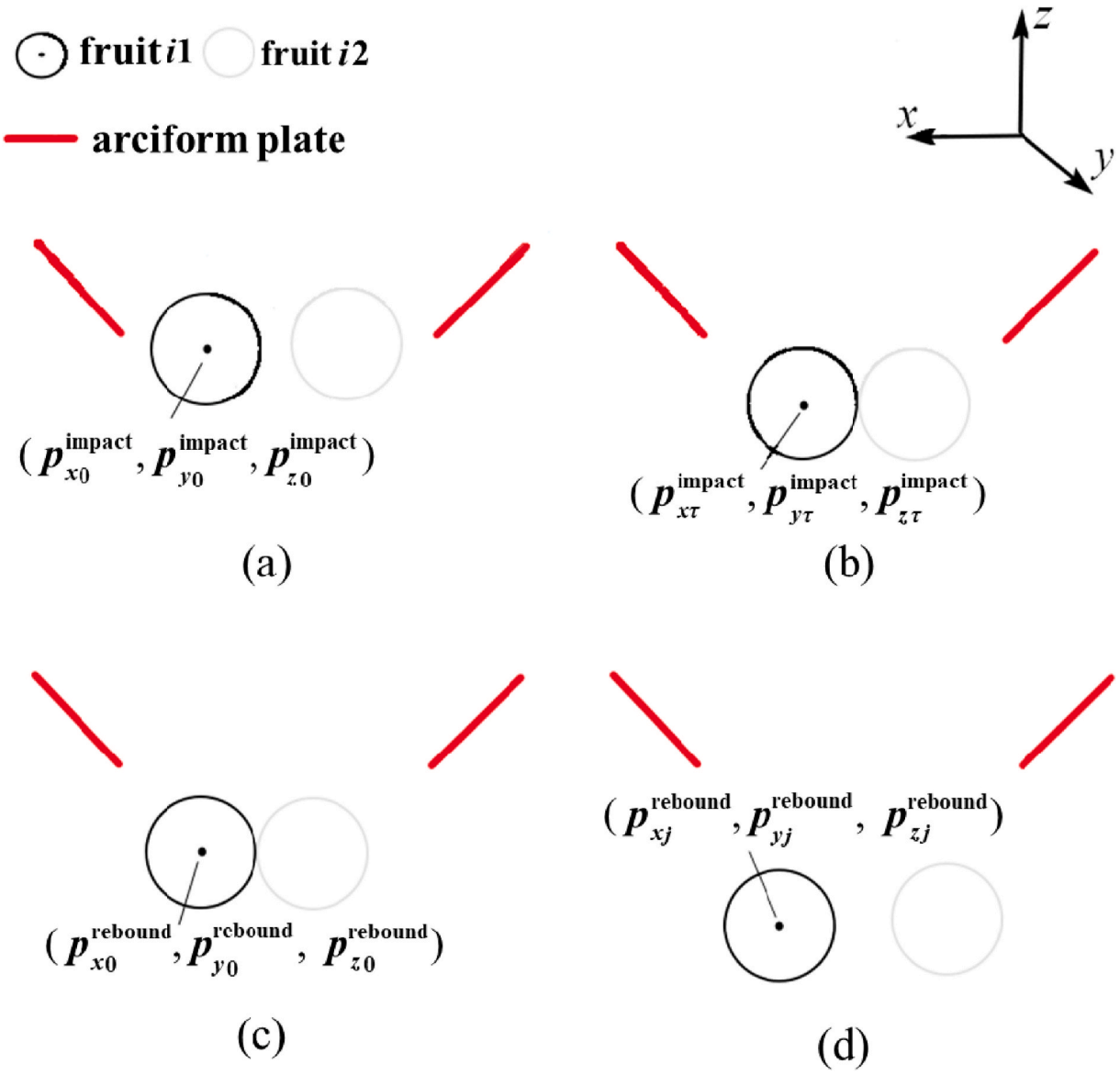


Fig. 4. Fruit displacements before and after collision. (a) Fruit initially leaving the arciform plate; (b) Fruit that impacted initially; (c) Fruit that rebounded initially; (d) Fruit moved for a period t_j after collision.

where i referred to serial number of the ith FFC test and t (from 0 to T) referred to the time of the deformation process during the collision; M_{i1} and M_{i2} referred to masses of fruit $i1$ and fruit $i2$, respectively; F_{i1} and F_{i2} referred to restoring forces of fruit $i1$ and fruit $i2$ during the collision, respectively.

(2) Impact and rebound velocities before and after collision

Both impact and rebound velocities were determined based on fruit displacements before and after the collision, which were used to calculate the CoR. Only the calculation processes of fruit $i1$ were described in this paper, since it was the same as that of fruit $i2$. As shown in Fig. 4, coordinates of fruit initially leaving the arciform plate were defined as ($p$impact $x0$, $p$impact $y0$, $p$impact $z0$) and changed to ($p$impact $x\tau$, $p$impact $y\tau$, $p$impact $z\tau$) after the fruit moved for a period (t_τ). Impact velocities in x-, y-, and z-directions ($v$impact x, $v$impact y, $v$impact z) were calculated as Eqs. (10)–(12), respectively. Besides, impact velocity in y-direction was 0 m/s because fruit's movement was restricted by the arciform plate, which resulted in calculation of the impact velocity of fruit before the FFC, as shown in Eq. (13). Similarly, coordinates of the fruit that rebounded initially were defined as ($p$rebound $_{x0}$, $p$rebound $_{y0}$, $p$rebound $_{z0}$) and altered to ($p$rebound $_{xj}$, $p$rebound $_{yj}$, $p$rebound $_{zj}$) after the fruit moved downwards for a period (t_j). Rebound velocities in x- and y-directions ($v$rebound $_x$, $v$rebound $_y$) were calculated as Eqs. (14) and (15), respectively. However, calculation of the rebound velocity in the z-direction ($v$rebound $_z$) needed to avoid influence of gravity, as shown in Eq. (16). Therefore, rebound velocity of fruit after the collision was calculated as Eq. (17).

$$v_x^{\text{impact}} = \frac{p_{x\tau}^{\text{impact}} - p_{x0}^{\text{impact}}}{t_\tau} \tag{10}$$

$$v_y^{\text{impact}} = \frac{p_{y\tau}^{\text{impact}} - p_{y0}^{\text{impact}}}{t_\tau} \tag{11}$$

$$v_z^{\text{impact}} = \frac{p_{z\tau}^{\text{impact}} - p_{z0}^{\text{impact}}}{t_\tau} + \frac{gt_\tau}{2} \tag{12}$$

$$v^{\text{impact}} = \sqrt{\left(v_x^{\text{impact}}\right)^2 + \left(v_z^{\text{impact}}\right)^2} \tag{13}$$

$$v_x^{\text{rebound}} = \frac{p_{xj}^{\text{rebound}} - p_{x0}^{\text{rebound}}}{t_j} \tag{14}$$

$$v_y^{\text{rebound}} = \frac{p_{yj}^{\text{rebound}} - p_{y0}^{\text{rebound}}}{t_j} \tag{15}$$

$$v_z^{\text{rebound}} = \frac{p_{zj}^{\text{rebound}} - p_{z0}^{\text{rebound}}}{t_j} - \frac{gt_j}{2} \tag{16}$$

$$v^{\text{rebound}} = \sqrt{\left(v_x^{\text{rebound}}\right)^2 + \left(v_y^{\text{rebound}}\right)^2 + \left(v_z^{\text{rebound}}\right)^2} \tag{17}$$

where x, y, and z referred to the x-, y- and z-directions of three-dimensional coordinate system, respectively; τ and j referred to the number of the frame in the FFC recorded by the high-speed digital camera; and g referred to the acceleration of gravity (9.81 m/s^2).

2.3.4. FFC test design

Ripening time and collision velocity v were selected as FFC test factors. The FFC was carried out with different ripening time (Day 0, Day 4, Day 8) and different collision velocities (1.1, 1.3, 1.5, 1.7, and 1.9 m/s) (Du et al., 2019; Xia et al., 2020). Collision angle was fixed at 35° to ensure fruit slide along with the arciform plate. Five repetitions were performed for each collision velocity. In addition, the amount of the kinetic energy of the fruit during the FFC may be absorbed by the rotational motion, which represents a small but significant contribution to the energy balance (Dattola et al., 2021; Kharaz et al., 2001; Yu et al., 2021). Therefore, an extra 20 repetitions (ripening time and collision velocity were fixed at Day 4 and 1.5 m/s, respectively) were performed to investigate the effect of rotation angle of fruit after the collision on the CoR. Each fruit, labelled according to the factors and number of tests, was only collided once to avoid the interference with measurement of the fruit damage from multiple collisions.

2.4. Fruit damage measurement

Total bruise volume (TBV), the sum of two fruit bruise volumes, was chosen to describe level of the fruit damage. Fruit samples were left on the lab bench at 25 °C for 48 h after FFC tests to allow color features of bruising to become more visible. As shown in Fig. 5, fruit were peeled to get bruise surface area, and then were cut into two equal parts in the direction of stem-calyx axis to obtain bruise depth profile (Opara and Pathare, 2014). Both the bruise surface area and the depth profile were circled by enclosed red solid lines, as shown in Fig. 5. The bruise surface area S_{elli} was assumed to be an elliptical shape, which was estimated by Eq. (13) after measuring major and minor axes of bruised surface. In this estimation model, the bruise volume V_{k} was described as a section of ellipsoid based on the full depth and it was estimated as Eq. (14). Both axial of bruise surface and depth profile were measured by a caliper.

$$S_{\text{elli}} = \frac{\pi}{4} w_1 w_2 \tag{18}$$

$$V_{\text{k}} = \frac{\pi d_{\text{b}}}{24}\left(3w_1 w_2 + 4{d_{\text{b}}}^2\right) \tag{19}$$

where w_1 referred to the major axis of bruised surface (mm); w_2 referred to the minor axis of bruised surface (mm); and d_{b} referred to the depth of bruise profile (mm).

3. Results and discussions

3.1. Kiwifruit firmness

With ripening of fruit, firmness decreased significantly and its standard deviation increased at the same ripening time. It was the highest on Day 0 and decreased with ripening, as shown in Table 1. Compared with Day 0, the fruit firmness decreased by 20.23% and 43.35% on Day 4 and Day 8, respectively. Initial slow and rapid softening phases have often been described the firmness change of kiwifruit with ripening (Burdon et al., 2017; Schröder and Atkinson, 2006). During storage, the initial slow softening phase was seen only in less ripe kiwifruit (Burdon et al., 2017). Therefore, kiwifruits from Day 0 to Day 4 were in the initial slow softening phase and their firmness decreased slowly. Subsequently, the accumulation of ethylene produced by kiwifruits increased with ripening, which accelerated physiological mechanisms of fruit (including the disassembly of polysaccharide networks in cell walls, pectin degradation, hydrolysis of starch celluloses and hemicellulose) and made them enter the rapid softening phase (Gong et al., 2020; Krupa and Tomala, 2021; Na et al., 2021; Oh et al., 2021). Kiwifruits from Day 4 to Day 8 were in the rapid softening phase and their firmness decreased rapidly. Standard deviation of the fruit firmness in the same group increased with ripening, which on Day 0, Day 4, and Day 8 were 10.98%, 26.09%, and 44.90% of the mean, respectively. Similar result had also been reported by Burdon et al. (2021) and Gwanpua et al. (2022). This may be caused by differences from ethylene production in different parts of kiwifruit during postharvest ripening (Na et al., 2021). Hence, inconsistency of the fruit firmness at the same ripening time became more obvious with ripening.

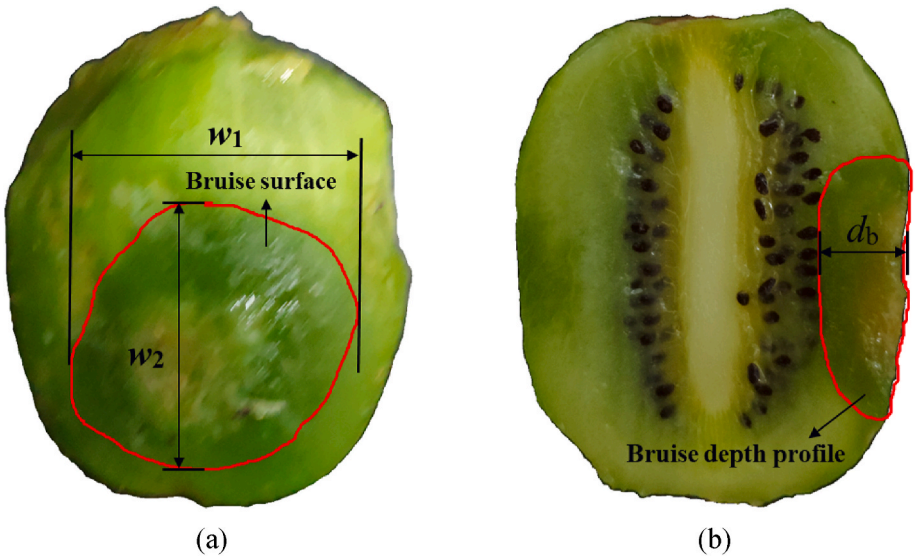


Fig. 5. Schematic diagram of fruit damage measurement after peeling skin. (a) The surface area; (b) The depth profile.

Table 1
Firmness of kiwifruits in the three ripening time (Mean ± standard deviation).

Ripening time (Day)	0	4	8
Firmness (gf)	17.3 ± 1.9[a]	13.8 ± 3.6[b]	9.8 ± 4.4[c]

Different letters indicated significant differences of firmness between ripening time ($p \leq 0.05$).

3.2. CoR of FFC

3.2.1. CoR of FFC in different ripeness

At the same collision velocity, the CoR on Day 0 and Day 4 were both large and their standard deviation was small, but on Day 8 was opposite. Deformation recovery ability of fruit tissue during the FFC declined with ripening, which made the fruit to absorb more collision energy and the CoR to decrease. This agreed with the finding of Wang et al. (2009) on peaches. Both starch and pectin depolymerized gradually with ripening, which increases intercellular space (Wang et al., 2021). Then more collision energy is absorbed by fruit during the FFC. However, the CoR on Day 0 was not significantly larger than that on Day 4 at the same collision velocity, which indicated that difference in the fruit firmness between Day 0 and Day 4 had no significant effect on the CoR. This may be due to some biological characteristics, such as the change of kiwifruit hair with ripening, which need to be studied in the future. In fact, whether hair on kiwifruit is related to its cultivar. For example, "Hayward" (Yin et al., 2009) and "Hongyang" (Du et al., 2019) are two common kiwifruit cultivars with and without fruit hair, respectively. Similarly, at the same collision velocity, standard deviation of the CoR on Day 0 and Day 4 were similar and both of them account for less than 12% of the mean, as shown in Fig. 6. The CoR is one of the most important input parameters of simulation, and its standard deviation usually needs to be less than 20% of the mean (González-Montellano et al., 2012; Saracoglu et al., 2012; Wang et al., 2020). Hence, the standard deviation of the CoR on Day 8 accounted for nearly 50% of the mean, which made the CoR on Day 8 unsuitable as a basis for simulation.

3.2.2. CoR of FFC in different collision velocities

Due to effect of collision force on the fruit deformation during the FFC, the CoR of the FFC decreased with collision velocity increasing, except for Day 8. The CoR of the FFC decreased with collision velocity increasing at Day 0 or Day4, as shown in Fig. 6, because of collision force increased with collision velocity increasing. The fruit deformation increased with collision force increasing, which caused an increase in energy loss and a decrease in the CoR of the FFC. Similar results have been found for apples (Stropek and Gołacki, 2016), pears (Stropek and

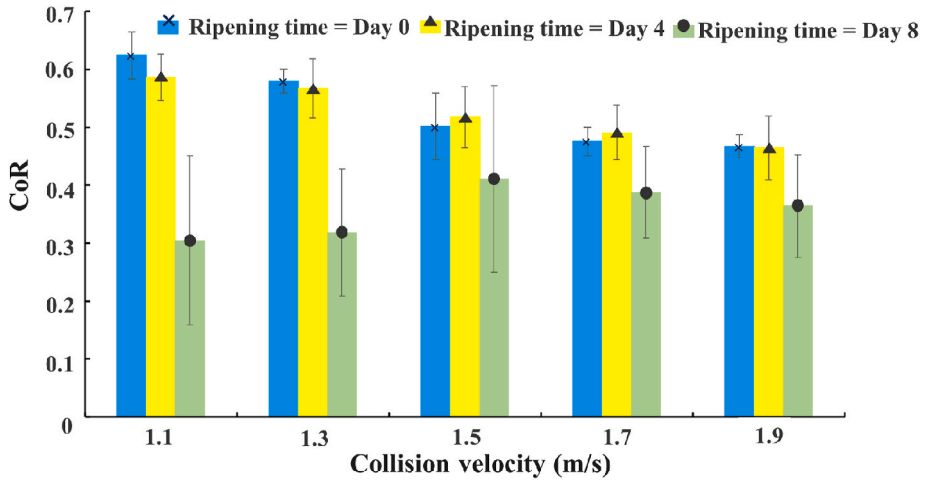


Fig. 6. The CoR of the FFC versus collision velocity.

Gołacki, 2019), and tomatoes (Van Zeebroeck et al., 2007b). However, based on the pendulum method, Ramírez-Gómez et al. (2014) found that particle-particle CoR of some biomass materials (rape straw, rice husk, maize stalk, sawdust and cereal straw, and maize stalk mixed with pine wood chips) increased with collision velocity increasing. This result may be caused by the interference of the binding force of string on the particle-particle collision. In the future, the CoR of kiwifruit needs to be studied by the pendulum method (Ahmadi et al., 2012; Zhu et al., 2016) or the drop method (Pang et al., 1992; Stropek and Gołacki, 2013), and results of which can measure the influence of introducing other colliding objects on the FFC. At Day 8, due to large deviation of the fruit firmness, the difference in the deformation between fruit was large when the velocities of fruit collision were the same. Therefore, the regularity of the CoR of the FFC on Day 8 with increasing of collision velocity was not obvious.

3.2.3. CoR of FFC with different fruit collision postures

According to the difference in the location of fruit at the collision point during the FFC, there were two types of fruit collision postures. Movement of fruit on arciform plate would impacted by the friction between kiwifruit and arciform plate when the kiwifruit slid on the arciform plate. There were slight differences in the velocities of the fruit due to friction as the fruit slide along the arciform plates, which leaded to slight difference in collision positions of the fruit. Fruit collision postures were classified into two types from the large number of experiments, which included 'calyx' - 'calyx' ('C' - 'C') and 'fruit body' - 'calyx' ('FB' - 'C'), as shown in Fig. 7.

The CoR was influenced by rotation angle of fruit during the collision due to the difference in fruit collision postures. The FFC began at $t = 0$ s and the images of moving fruit after collision were obtained every 0.007 s. Different fruit collision postures resulted in different rotation angles for each fruit, as shown by black arrows in Fig. 8, where white and yellow dotted lines showed fruit's initial locations and their positions after collision, respectively. CoRs were different due to influence of rotation angles of collision position. For instance, the CoR of FFC was 0.491 when the rotation angles of two fruit were both more than 13°. And the CoR of FFC was 0.528 when the rotation angles of two fruit were both less than 8°, as shown in Fig. 8. Therefore, it could be deduced that the CoR of FFC decreased with the rotation angles of the fruit increasing. However, the CoR in rotational direction was not considered in this paper, because the theoretical formula of the CoR belonged to kinematic definition and did not involve the effect of the rotational direction on the energy change during the FFC. There are three definitions for the CoR: kinematic, kinetic, and energetic (Minamoto and Kawamura, 2009). Compared with kinematic and kinetic, Ivanov (1992) found that the energetic definition of the CoR is more suitable for eccentric collision with friction. Hence, the theoretical formula of the CoR could be deduced based on energetic in the future.

3.3. Damage of fruit

The fruit damage decreased with the CoR increasing, because an increase in the CoR could imply a decrease in the collision energy absorbed by the fruit during the FFC. According to formula of the CoR, fruit with larger CoR suffered less damage, because it means that the fruit absorbs less collision energy during the FFC. CoRs of fruit on Day 0 and Day 4 were mostly in the range of 0.45–0.7, while the TBV was mostly lower than 20,000 mm^3, as shown in Fig. 9. In addition, due to significant inconsistency of the fruit firmness, the range of the CoR and the TBV on the Day 8 were also larger than those of other ripening time, which were 0.11–0.52 and 2000–35000 mm^3, respectively. These results were highly correlated with the previous experimental findings that correlations were observed between the CoR and the fruit damage (Pang et al., 1992; Stropek and Gołacki, 2016, 2019). In this study, axial of bruise surface and depth profile were measured by a caliper. However, it may be more efficient to determine the bruise surface area of the fruit photographed at a fixed distance through image processing (Komarnicki et al., 2017a, 2017b; Stopa et al., 2018). All fruit were damaged on Day 8 because the fruit deformation was large and not easily recovered during the FFC. And the lowest CoR without the fruit damage increased with ripening, which on Day 0 and Day 4 were 0.47 and 0.58, respectively. It is also important for the design of fresh kiwifruit processing equipment in orchards, where mechanical damage may cause fruit quality downgrading (An et al., 2020; Du et al., 2019). Therefore, the CoR could not only be an appropriate parameter to predict the fruit damage, but also provide guidance for the design of orchard equipment.

4. Conclusions

The FFC without introducing other colliding objects in different ripeness was achieved by designing a special platform, where ripening time, collision velocity, and fruit collision postures had effect on the CoR. Fruit more ripening has lower firmness, which were easier to absorb larger collision energy during the FFC. Similarly, due to effect of collision force on the fruit during the FFC, the collision energy absorbed by the fruit increased with collision velocity increasing. However, although the fruit absorbing more collision energy means a decrease in the CoR, the small decrease in the fruit firmness in early stage of ripening has no significant effect on the CoR. In addition, under the same collision velocity, the CoR of the 'C' - 'C' collision posture was smaller than of the 'FB' - 'C' collision posture because the difference in the rotation angle of the fruit during the FFC. The CoR exceeding 0.58 on early ripening time could be used for simulation, because there was no fruit damage and the standard deviation of the CoR was small. Conversely, the CoR with late ripening time could not be the basis for simulation parameters because standard deviation as a percentage of the mean will increase with ripening. A strong correlation was found between the CoR and the TBV, despite the CoR at the beginning of the fruit damage increased with ripening. This result suggests that the CoR could be an appropriate parameter for predicting the fruit damage. The CoR

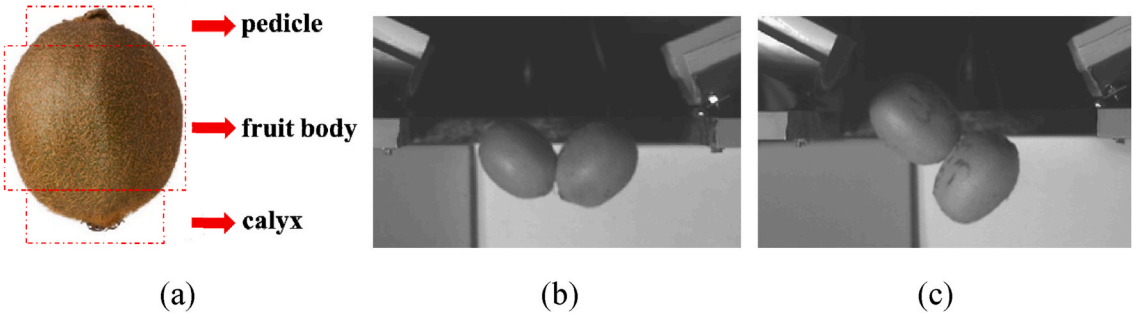


Fig. 7. Fruit area division and two fruit collision postures. (a) Fruit location division; (b) 'C' - 'C' collision posture; (c) 'FB' - 'C' collision posture.

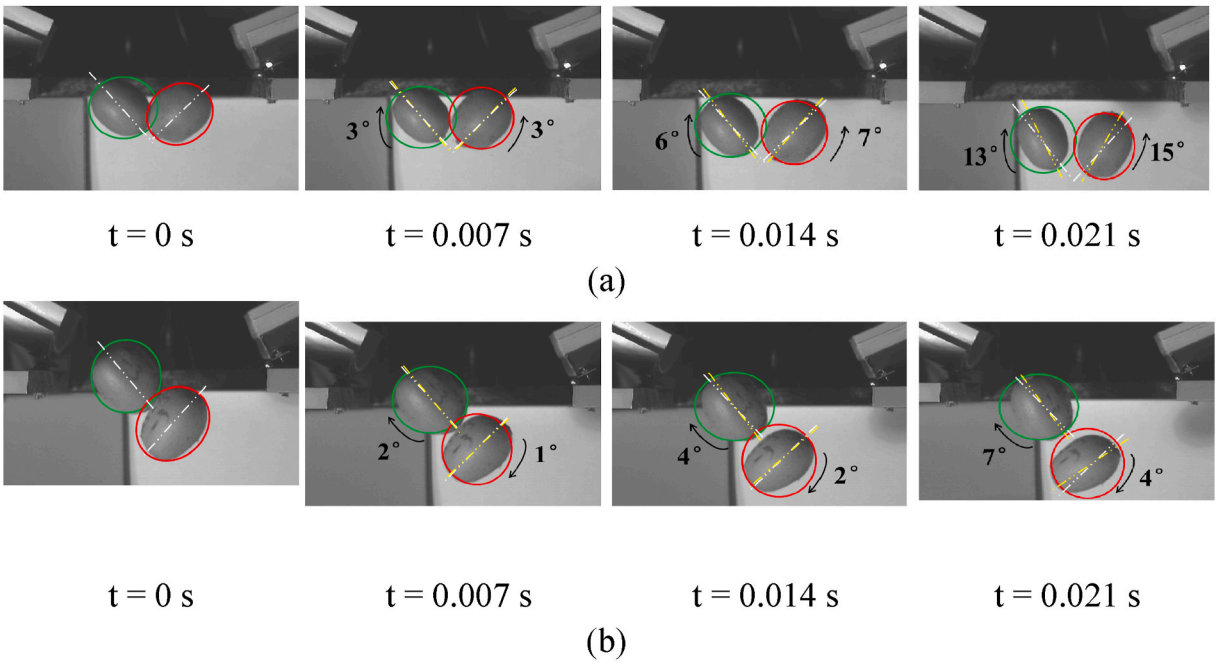


Fig. 8. Rotation process of fruit after the collision in different fruit collision postures (Ripening time = Day 4, collision velocity = 1.5 m/s). (a) 'C' - 'C' collision posture (CoR = 0.491); (b) 'FB' - 'C' collision posture (CoR = 0.528).

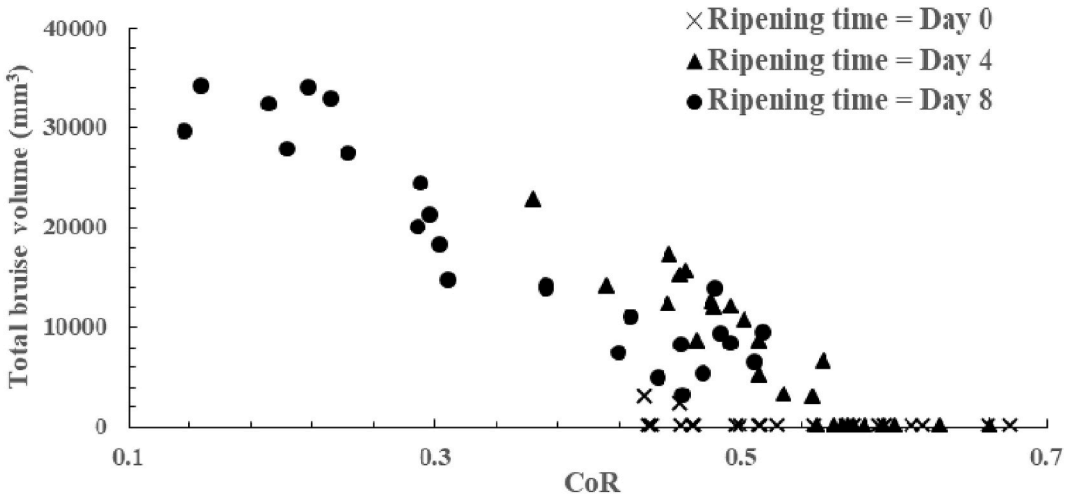


Fig. 9. Total bruise volume (TBV) versus the CoR of FFC.

can not only be an indicator to determine the degree of the fruit damage, but also study motion characteristics of fruit without mechanical damage by simulation, which is helpful to develop harvesting, handling and transporting equipment.

Credit author statement

Zhenchao Wu: Conceptualization, Writing – original draft preparation. Guo Li: Methodology, Validation. Ruizhe Yang: Visualization, Investigation. Longsheng Fu: Supervision, Writing- Reviewing and Editing. Rui Li: Investigation, Project administration. Shaojin Wang: Writing- Reviewing and Editing,

Declaration of competing interest

The authors declare that they have no known competing financial interests or personal relationships that could have appeared to influence the work reported in this paper.

Acknowledgements

This work was partially supported by the National Natural Science Foundation of China (32171897); Science and Technology Program in Yulin City of China (CXY-2020-076); Youth Science and Technology Nova Program in Shaanxi Province of China (2021KJXX-94); China Postdoctoral Science Foundation funded project (2021M692656); Recruitment Program of High-End Foreign Experts of the State Administration of Foreign Experts Affairs, Ministry of Science and Technology, China (G20200027075).

References

Ahmadi, E., Ghassemzadeh, H.R., Sadeghi, M., Moghaddam, M., Neshat, S.Z., Ettefagh, M.M., 2012. Dynamic modeling of peach fruit during normal impact.

J. Food Process. Eng. 35, 483–504. https://doi.org/10.1111/j.1745-4530.2010.00603.x.
An, X., Li, Z., Zude-Sasse, M., Tchuenbou-Magaia, F., Yang, Y., 2020. Characterization of textural failure mechanics of strawberry fruit. J. Food Eng. 282, 110016. https://doi.org/10.1016/j.jfoodeng.2020.110016.
Bader, F., Rahimifard, S., 2020. A methodology for the selection of industrial robots in food handling. Innovat. Food Sci. Emerg. Technol. 64, 102379. https://doi.org/10.1016/j.ifset.2020.102379.
Barnabé, M., Blanc, N., Chabin, T., Delenne, J.Y., Duri, A., Frank, X., Hugouvieux, V., Lutton, E., Mabille, F., Nezamabadi, S., Perrot, N., Radjai, F., Ruiz, T., Tonda, A., 2018. Multiscale modeling for bioresources and bioproducts. Innovat. Food Sci. Emerg. Technol. 46, 41–53. https://doi.org/10.1016/j.ifset.2017.09.015.
Burdon, J., Martin, P., Ireland, H., Schaffer, R., McAtee, P., Boldingh, H., Nardozza, S., 2021. Transcriptomic analysis reveals differences in fruit maturation between two kiwifruit cultivars. Sci. Hortic. 286, 110207. https://doi.org/10.1016/j.scienta.2021.110207.
Burdon, J., Pidakala, P., Martin, P., Billing, D., 2017. Softening of 'Hayward'' kiwifruit on the vine and in storage: the effects of temperature. ' Sci. Hortic. 220, 176–182. https://doi.org/10.1016/j.scienta.2017.04.004.
Dattola, G., Crosta, G.B., di Prisco, C., 2021. Investigating the influence of block rotation and shape on the impact process. Int. J. Rock Mech. Min. Sci. 147, 104867. https://doi.org/10.1016/j.ijrmms.2021.104867.
Delpino-Rius, A., Marsol-Vall, A., Eras, J., Llovera, M., Cubero, M.Á., Balcells, M., Canela-Garayoa, R., 2018. Bulk industrial fruit fibres. Characterization and prevalence of the original fruit metabolites. Food Res. Int. 111, 1–10. https://doi.org/10.1016/j.foodres.2018.05.001.
Du, D., Wang, B., Wang, J., Yao, F., Hong, X., 2019. Prediction of bruise susceptibility of harvested kiwifruit (Actinidia chinensis) using finite element method. Postharvest Biol. Technol. 152, 36–44. https://doi.org/10.1016/j.postharvbio.2019.02.013.
Fu, H., Karkee, M., He, L., Duan, J., Li, J., Zhang, Q., 2020. Bruise patterns of fresh market apples caused by fruit-to-fruit impact. Agronomy 10, 59. https://doi.org/10.3390/agronomy10010059.
Gong, H.J., Fullerton, C., Billing, D., Burdon, J., 2020. Retardation of 'Hayward' kiwifruit tissue zone softening during storage by 1-methylcyclopropene. Sci. Hortic. 259, 108791. https://doi.org/10.1016/j.scienta.2019.108791.
González-Montellano, C., Fuentes, J.M., Ayuga-Téllez, E., Ayuga, F., 2012. Determination of the mechanical properties of maize grains and olives required for use in DEM simulations. J. Food Eng. 111, 553–562. https://doi.org/10.1016/j.jfoodeng.2012.03.017.
Gwanpua, S.G., Zhao, M., Jabbar, A., Bronlund, J.E., East, A.R., 2022. A model for firmness and low temperature-induced storage breakdown disorder of 'Hayward' kiwifruit in supply chain. Postharvest Biol. Technol. 185, 111789. https://doi.org/10.1016/j.postharvbio.2021.111789.
Ivanov, A.P., 1992. Energetics of a collision with friction. J. Appl. Math. Mech. 56, 527–534. https://doi.org/10.1016/0021-8928(92)90008-V.
Kanakabandi, C.K., Goswami, T.K., 2019. Determination of properties of black pepper to use in discrete element modeling. J. Food Eng. 246, 111–118. https://doi.org/10.1016/j.jfoodeng.2018.11.005.
Kharaz, A.H., Gorham, D.A., Salman, A.D., 2001. An experimental study of the elastic rebound of spheres. Powder Technol 120, 281–291. https://doi.org/10.1016/S0032-5910(01)00283-2.
Komarnicki, P., Stopa, R., Kuta, Ł., Szyjewicz, D., 2017a. Determination of apple bruise resistance based on the surface pressure and contact area measurements under impact loads. Comput. Electron. Agric. 142, 155–164. https://doi.org/10.1016/j.compag.2017.08.028.
Komarnicki, P., Stopa, R., Szyjewicz, D., Kuta, Ł., Klimza, T., 2017b. Influence of contact surface type on the mechanical damages of apples under impact loads. Food Bioprocess Technol 10, 1479–1494. https://doi.org/10.1007/s11947-017-1918-z.
Krupa, T., Tomala, K., 2021. Effect of oxygen and carbon dioxide concentration on the quality of minikiwi fruits after storage. Agronomy 11, 2251. https://doi.org/10.3390/agronomy11112251.
Lu, F., Ishikawa, Y., Kitazawa, H., Satake, T., 2010. Measurement of impact pressure and bruising of apple fruit using pressure-sensitive film technique. J. Food Eng. 96, 614–620. https://doi.org/10.1016/j.jfoodeng.2009.09.009.
Minamoto, H., Kawamura, S., 2009. Effects of material strain rate sensitivity in low speed impact between two identical spheres. Int. J. Impact Eng. 36, 680–686. https://doi.org/10.1016/j.ijimpeng.2008.10.001.
Na, L., Yao, C., Chen, Y., Ping, Z., Guofang, X., 2021. Ripening and ethylene production affected by 1-MCP in different parts of kiwifruit during postharvest storage. Int. J. Food Prop. 24, 1011–1021. https://doi.org/10.1080/10942912.2021.1953071.
Oh, T.G., Jo, J.A., Lee, S.J., 2021. Evaluation of time–temperature integrator for indicating the ripeness of kiwifruit in plastic container at home. J. Food Sci. 86, 2872–2885. https://doi.org/10.1111/1750-3841.15795.
Opara, L.U., Al-Ghafri, A., Agzoun, H., Al-Issai, J., Al-Jabri, F., 2007. Design and development of a new device for measuring susceptibility to impact damage of fresh produce. N. Z. J. Crop Hortic. Sci. 35, 245–251. https://doi.org/10.1080/01140670709510191.
Opara, L.U., Pathare, P.B., 2014. Bruise damage measurement and analysis of fresh horticultural produce-A review. Postharvest Biol. Technol. 91, 9–24. https://doi.org/10.1016/j.postharvbio.2013.12.009.
Pang, W., Studman, C.J., Ward, G.T., 1992. Bruising damage in apple-to-apple impact. J. Agric. Eng. Res. 52, 229–240. https://doi.org/10.1016/0021-8634(92)80063-X.
Ramírez-Gómez, Á., Gallego, E., Fuentes, J.M., González-Montellano, C., Ayuga, F., 2014. Values for particle-scale properties of biomass briquettes made from agroforestry residues. Particuology 12, 100–106. https://doi.org/10.1016/j.partic.2013.05.007.
Rojas, M.L., Leite, T.S., Cristianini, M., Alvim, I.D., Augusto, P.E.D., 2016. Peach juice processed by the ultrasound technology: changes in its microstructure improve its physical properties and stability. Food Res. Int. 82, 22–33. https://doi.org/10.1016/j.foodres.2016.01.011.
Rossow, J., Coetzee, C.J., 2021. Discrete element modelling of a chevron patterned conveyor belt and a transfer chute. Powder Technol 391, 77–96. https://doi.org/10.1016/j.powtec.2021.06.012.
Saracoglu, T., Ucer, N., Ozarslan, C., 2012. Selected geometric characteristics, hydrodynamic properties, and impact parameters of quince fruit (Cydonia vulgaris Pers.). Int. J. Food Prop. 15, 758–769. https://doi.org/10.1080/10942912.2010.501468.
Schröder, R., Atkinson, R.G., 2006. Kiwifruit cell walls: towards an understanding of softening? New Zeal. J. For. Sci. 36, 112–129.
Stopa, R., Szyjewicz, D., Komarnicki, P., Kuta, Ł., 2018. Determining the resistance to mechanical damage of apples under impact loads. Postharvest Biol. Technol. 146, 79–89. https://doi.org/10.1016/j.postharvbio.2018.08.016.
Stropek, Z., Gołacki, K., 2019. Impact characteristics of pears. Postharvest Biol. Technol. 147, 100–106. https://doi.org/10.1016/j.postharvbio.2018.09.015.
Stropek, Z., Gołacki, K., 2016. Quantity assessment of plastic deformation energy under impact loading conditions of selected apple cultivars. Postharvest Biol. Technol. 115, 9–17. https://doi.org/10.1016/j.postharvbio.2015.12.011.
Stropek, Z., Gołacki, K., 2013. The effect of drop height on bruising of selected apple varieties. Postharvest Biol. Technol. 85, 167–172. https://doi.org/10.1016/j.postharvbio.2013.06.002.
Studman, C.J., Brown, G.K., Timm, E.J., Schulte, N.L., Vreede, M.J., 1997. Bruising on blush and non-blush sides in apple-to-apple impacts. Trans. Am. Soc. Agric. Eng. 40, 1655–1663. https://doi.org/10.13031/2013.21405.
Tan, Y., Yu, Y., Fottner, J., Kessler, S., 2021. Automated measurement of the numerical angle of repose (aMAoR) of biomass particles in EDEM with a novel algorithm. Powder Technol 388, 462–473. https://doi.org/10.1016/j.powtec.2021.04.062.
Van Zeebroeck, M., Lombaert, G., Dintwa, E., Ramon, H., Degrande, G., Tijskens, E., 2008. The simulation of the impact damage to fruit during the passage of a truck over a speed bump by means of the discrete element method. Biosyst. Eng. 101, 58–68. https://doi.org/10.1016/j.biosystemseng.2008.06.003.
Van Zeebroeck, M., Tijskens, E., Dintwa, E., Kafashan, J., Loodts, J., De Baerdemaeker, J., Ramon, H., 2006. The discrete element method (DEM) to simulate fruit impact damage during transport and handling: case study of vibration damage during apple bulk transport. Postharvest Biol. Technol. 41, 92–100. https://doi.org/10.1016/j.postharvbio.2006.02.006.
Van Zeebroeck, M., Van linden, V., Darius, P., De Ketelaere, B., Ramon, H., Tijskens, E., 2007a. The effect of fruit factors on the bruise susceptibility of apples. Postharvest Biol. Technol. 46, 10–19. https://doi.org/10.1016/j.postharvbio.2007.03.017.
Van Zeebroeck, M., Van linden, V., Darius, P., De Ketelaere, B., Ramon, H., Tijskens, E., 2007b. The effect of fruit properties on the bruise susceptibility of tomatoes. Postharvest Biol. Technol. 45, 168–175. https://doi.org/10.1016/j.postharvbio.2006.12.022.
Wang, H., Wang, J., Mujumdar, A.S., Jin, X., Liu, Z.L., Zhang, Y., Xiao, H.W., 2021. Effects of postharvest ripening on physicochemical properties, microstructure, cell wall polysaccharides contents (pectin, hemicellulose, cellulose) and nanostructure of kiwifruit (Actinidia deliciosa). Food Hydrocolloids 118, 106808. https://doi.org/10.1016/j.foodhyd.2021.106808.
Wang, L., Wu, B., Wu, Z., Li, R., Feng, X., 2018. Experimental determination of the coefficient of restitution of particle-particle collision for frozen maize grains. Powder Technol 338, 263–273. https://doi.org/10.1016/j.powtec.2018.07.005.
Wang, L., Zheng, Z., Yu, Y., Liu, T., Zhang, Z., 2020. Determination of the energetic coefficient of restitution of maize grain based on laboratory experiments and DEM simulations. Powder Technol 362, 645–658. https://doi.org/10.1016/j.powtec.2019.12.024.
Wang, W., Lu, H., Zhang, S., Yang, Z., 2019. Damage caused by multiple impacts of litchi fruits during vibration harvesting. Comput. Electron. Agric. 162, 732–738. https://doi.org/10.1016/j.compag.2019.04.037.
Wang, Y.W., Wang, J., Yao, C., Lu, Q.J., 2009. Firmness measurement of peach by impact force response. J. Zhejiang Univ. - Sci. B 10, 883–889. https://doi.org/10.1631/jzus.B0920108.
Wu, Z., Yang, R., Gao, F., Wang, W., Fu, L., Li, R., 2021. Segmentation of abnormal leaves of hydroponic lettuce based on DeepLabV3+ for robotic sorting. Comput. Electron. Agric. 190, 106443. https://doi.org/10.1016/j.compag.2021.106443.
Xia, M., Zhao, X., Wei, Xiaopeng, Guan, W., Wei, Xiaobo, Xu, C., Mao, L., 2020. Impact of packaging materials on bruise damage in kiwifruit during free drop test. Acta Physiol. Plant. 42, 119. https://doi.org/10.1007/s11738-020-03081-5.
Yin, X., ren, Allan, A.C., Zhang, B., Wu, R. mei, Burdon, J., Wang, P., Ferguson, I.B., Chen, K. song, 2009. Ethylene-related genes show a differential response to low temperature during "Hayward" kiwifruit ripening. Postharvest Biol. Technol. 52, 9–15. https://doi.org/10.1016/j.postharvbio.2008.09.016.
Yu, Z., Hu, Z., Peng, B., Gu, F., Yang, L., Yang, M., 2021. Experimental determination of restitution coefficient of garlic bulb based on high-speed photography. Int. J. Agric. Biol. Eng. 14, 81–90. https://doi.org/10.25165/J.IJABE.20211402.5882.
Zhao, J., Sugirbay, A., Liu, F., Chen, Y., Hu, G., Zhang, E., Chen, J., 2019. Parameter optimization of winnowing equipment for machine-harvested Lycium barbarum L. Spanish J. Agric. Res. 17, e0203 https://doi.org/10.5424/sjar/2019172-14449.
Zhu, Q., Guan, J., Huang, M., Lu, R., Mendoza, F., 2016. Predicting bruise susceptibility of "Golden Delicious" apples using hyperspectral scattering technique. Postharvest Biol. Technol. 114, 86–94. https://doi.org/10.1016/j.postharvbio.2015.12.007.